

Spatial gradients enhance persistence of hypercycles

Maarten C. Boerlijst¹, Pauline Hogeweg

Theoretical Biology Group, Utrecht University, Padualaan 8, 3584 CH Utrecht, The Netherlands

Received 12 October 1994; revised 10 March 1995; accepted 24 March 1995

Communicated by A.C. Newell

Abstract

In this paper we study a partial differential equation model of cyclic catalysis of replicating entities (i.e. a hypercycle). In the presence of a spatial gradient in the decay rate of molecules we observe spiral drift towards the region of faster rotating spirals. On a radial gradient one spiral anchors in the region of fastest rotation. If the drop in the gradient is large enough, this spiral will break up in the periphery and form new spiral centres. The system settles in a dynamic equilibrium.

This equilibrium turns out to be persistent even against strong parasites, i.e., molecules that receive increased catalysis but do not give any catalysis. If just one peripheral spiral manages to escape the first attacking wave of the parasite, this spiral will gradually push out the parasites and in the long run the dynamic equilibrium will be completely restored. We conclude that a gradient can supply regenerative power to the hypercycle.

1. Introduction

The concept of a hypercycle was introduced in the early seventies (Eigen 1971) as a model for cyclic helping of self-replicating entities. Fig. 1A shows a schematic diagram of a hypercycle: each member of the cycle supports the replication of the next member. Eigen and Schuster (1979, 1982; Eigen 1992) suggested that hypercycles of RNA molecules may have played a role in prebiotic evolution. They showed that in a system containing self-replicative molecules the length of the molecules is restricted by the accuracy of replication. The maximum length that the mole-

cules can attain by the process of Darwinian selection seems to be much too short to accumulate the information necessary to improve on the fidelity of replication (e.g. by coding for replicases). They call this the “information threshold”: there is too little information to permit an increase in the amount of information. Eigen and Schuster suggested that a hypercycle of

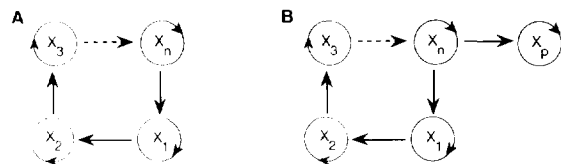


Fig. 1. Schematic diagram of a hypercycle. The hypercycle consists of n self-replicating molecule species X_i . (A) Each species provides catalytic support for the subsequent species in the cycle. (B) As (A), but now a parasitic species X_p is coupled to the hypercycle.

¹ Current address: Department of Zoology, University of Oxford, South Parks Road, Oxford OX1 3PS, United Kingdom.

RNA molecules that catalyse the replication of each other in a cyclic way could cross the information threshold. Each molecule species in the cycle is still bound to the maximum string length, but the molecules can combine their information and thus cross the threshold.

There are two major problems connected with this idea. The first problem is that hypercycles can contain only a small number of species. Hypercycles that consist of five or more species show limit cycle behaviour and the size of the limit cycle quickly expands with the number of species (Eigen and Schuster 1979; Hofbauer and Sigmund 1988). In a biological system this implies that large hypercycles will be unstable because some species will become extinct. It seems unlikely that a short hypercycle can contain the information necessary to cross the information threshold. The second problem is that the giving of catalytic support to another molecule is in fact an “altruistic” property and therefore the property will not be maintained (see e.g. Maynard Smith 1979). This is best demonstrated by the fact that hypercycles are vulnerable to so-called “parasites” (see Fig. 1B). A parasitic molecule receives catalysis from a molecule in the cycle, but it does not give any catalysis in return. If the parasite receives more catalysis than the competing species in the cycle (i.e. a “strong” parasite), it will first outcompete this species and finally the complete cycle will be lost. There seems to be a large class of parasites that are fatal to hypercycles, i.e. hypercycles are evolutionarily unstable.

In our earlier work on cellular automaton models of hypercycles (Boerlijst and Hogeweg 1991a,b) we have shown that spatial self-structuring completely solves the extinction problem and partially solves the parasite problem. In a spatial model hypercycles that consist of five or more species (there seems to be no upper limit) spontaneously generate spiral waves. Such a spiral wave is a rotating pattern of all species in the hypercycle and within a spiral wave global extinction of species no longer occurs (although

locally there is a continuous extinction and re-invasion process). Furthermore, spiral waves provide stability against parasites (Boerlijst and Hogeweg 1991a; May 1991). Spiral waves are resistant to parasite invasions that do not start near the centre of the spiral. If, however, the centre of a spiral is infected by parasites the entire spiral will be lost. As long as there are uninfected spirals the hypercycle will be maintained, but there is no regeneration of “killed” spirals. Thus the emergence of spiral waves reduces the parasite problem, but it does not completely solve it.

In this study we will show that in the presence of spatial heterogeneity a combination of resistance to parasites and regeneration of spirals can be achieved. We will introduce this heterogeneity in the form of a spatial gradient in the decay rate of molecules. From experimental and theoretical excitable media spirals it is known that spiral waves respond to gradients. Typically on a gradient the centre of a spiral will drift and thus the whole spiral will slowly move (e.g. Markus et al. 1992; Davidenko et al., 1992). Furthermore, spirals can break up into new spirals if the drop in the gradient is large enough (analogous to e.g. Yamaguchi and Müller 1991). In this paper we first show that these two effects of drift and break-up occur in the case of hypercycle spirals. Secondly, we will demonstrate the implications of a gradient for the stability of hypercycles against parasites. Finally we will discuss the situation of a medium with multiple gradients.

2. The model

In this section we present the partial differential equation (PDE) model that was used for numerical computations. The general results of this paper also hold for the cellular automaton (CA) model that we used in our earlier papers on hypercycles (Boerlijst and Hogeweg 1991a,b). The PDE-model is completely deterministic, the spiral waves are better behaved and easier to

study than in the stochastic CA-model. On the other hand, in the CA-model the individuals are well-defined, whereas in the PDE-model an explicit extinction threshold (and thus loss of mass) is necessary to prevent the diffusion of unrealistically small fractions (Durrett and Levin 1994).

2.1. Processes

Let X_i denote a molecule of type i , and let there be n types of molecules. In our model we want to include the following processes:

A. Decay of molecules



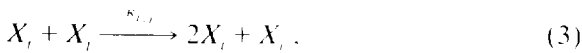
in which δ_i stands for the decay rate of molecule type i .

B. Non catalysed replication



in which ρ_i stands for the non-catalysed replication rate of molecule type i .

C. Catalysed replication



in which $\kappa_{i,j}$ stands for the rate of catalysed replication of molecule type i , which is catalysed by molecule type j .

D. Competition

In the original hypercycle model competition is modelled by assuming a chemostat, i.e., the total number of molecules is kept constant by introducing a flux which is equal to the average growth of the system at any given time. In our model we use a different kind of competition. We assume that the rate of replication is proportional to the fraction of “empty spots” (as in a cellular automaton model; see Toffoli and Mar-

golus 1987; Boerlijst and Hogeweg 1991a), which is equal to:

$$1 - \frac{\sum_{k=1}^n X_k}{N}, \quad (4)$$

in which N stands for the total number of spots available.

The reason for using this “carrying capacity” assumption instead of a chemostat assumption is that in the PDE model we want to make it possible for the local density of molecules to vary (for instance due to differences in the local amount of catalysis).

2.2. ODE (ordinary differential equation) model

The processes mentioned in Section 2.1 lead to the following ODE model:

$$\dot{X}_i = X_i \left(-\delta_i + \left\{ 1 - \sum_{k=1}^n X_k \right\} \{ \rho_i + \kappa_{i,i-1} X_{i-1} \} \right), \quad (5)$$

in which $i-1$ denotes the previous species in the cycle; note that we have got rid of N by scaling X_i to fractions.

As a default parameter setting for a hypercycle of n members we use:

$$\forall i: \delta_i = 0.05, \quad \rho_i = 0.1, \quad \kappa_{i,i-1} = 0.5. \quad (6)$$

The dynamics of this model resembles that of the chemostat hypercycle model (Hofbauer and Sigmund 1988; Eigen and Schuster 1979): hypercycles of 4 or less members attain a stable equilibrium, whereas hypercycles of 5 or more members show limit cycle behaviour. The size of the limit cycle quickly increases with the number of species in the cycle, so that for practical (biological) purposes some species will become extinct and the cycle will be lost. Note that for simple cases the ODE model corresponds to simple ecosystem models. For instance, for one species and no catalysis the model collapses to a model of a logistically growing population with carrying capacity $1 - \delta_i/\rho_i$. If there are more than

one species, but no catalysis, Eq. (5) collapses to a Lotka–Volterra model of competing species with complete niche overlap, a case of competitive exclusion (see e.g. McGehee and Armstrong 1977).

2.3. PDE model

In order to study the effects of spatial pattern formation on the dynamics and evolutionary properties of the hypercycle, we simply extend the ODE model (Eq. (5)) with a Laplacian operator ∇ :

$$\dot{X}_i = X_i \left(-\delta_i + \left\{ 1 - \sum_k X_k \right\} \{ \rho_i + \kappa_{i,i} \cdot X_i \} \right) + D \nabla^2 X_i, \quad (7)$$

For numerical computations we use the explicit Euler method with Neumann boundary conditions and a rectangular grid of 100×100 elements up to a maximum of 200×200 elements. X_i should be interpreted as the fraction of molecules of type i at a given grid point, and D is the diffusion coefficient. We use an explicit extinction level at a fraction of $X_i < 0.001$. The basic properties of the hypercycle spirals, such as

rotation speed and spiral tip dynamics, are hardly affected by this extinction level. Furthermore, the phenomena that are described in the next section (i.e. spiral break-up and spiral drift) do not depend on the explicit extinction. For e.g. resistance against parasites the explicit extinction is necessary, because otherwise the parasite would diffuse in unrealistically small fractions to every grid point and thus it would infect all spiral centres. The effects of spatial dependence of δ_i in Eq. (7) are the main subject of this paper.

3. Hypercycles on a decay gradient

In order to obtain a better understanding of the response of a hypercycle spiral to a decay gradient we first describe the behaviour of a spiral for different fixed values of the decay. Figs. 2A and B show superimposed pictures of one species in a hypercycle spiral in two different decay regimes. In Fig. 2A the decay rate is relatively small at $\forall i: \delta_i = 0.03$. The spiral has a large period of approximately 1,650 time steps. The tip of the spiral is rotating around a small circular core (as in Jahnke et al. 1989). In Fig. 2B the decay rate is much larger at $\forall i: \delta_i = 0.07$;

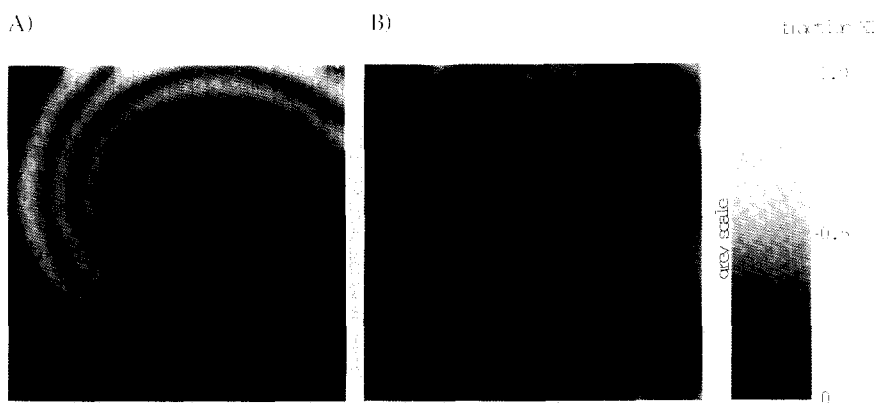


Fig. 2. A hypercycle spiral in two decay-regimes (A) Slow decay: $\forall i: \delta_i = 0.03$. (B) Fast decay: $\forall i: \delta_i = 0.07$. A hypercycle of twelve members is simulated in the PDE of Eq. (7) with the default parameters of Eq. (6) except for δ_i . For computation a grid of 100×100 elements is used with a time step of 1. The diffusion coefficient D equals 0.16. Both figures show three superposed images of the spiral arm of species X_1 with an interval of 200 time steps. The spiral in the fast decay regime rotates faster; it contains smaller fractions of all species and its tip rotates around a slightly larger circular core than the spiral in the slow decay regime.

the spiral is now rotating almost twice as fast, at a period of around 900 time steps, but its tip is rotating around a slightly larger core. The differences in period and in core size cause two gradient phenomena, namely break-up of spirals and drift of spirals. We will describe these phenomena in the next two sections.

3.1. Spiral break-up

If the drop in the gradient is large enough (i.e. if the difference in period between both sides of a gradient is large enough) a spiral will break up in the slower region. In Figs. 3a–d the right-hand side of the field has a homogeneous decay rate of ∇i : $\delta_i = 0.07$. Starting from the middle to the left-hand side of the field there is a smooth gradient from ∇i : $\delta_i = 0.07$ to ∇i : $\delta_i = 0.03$. In Fig. 3a a single spiral is initialised on the right-hand side of the field. Figs. 3b–d show that the spiral is unable to force its period through the slower region. This will first result in the collision of subsequent waves (Fig. 3b) which causes these waves to break (Fig. 3c). The process of colliding and breaking of waves will finally result in the formation of multiple spiral centres (Fig. 3d).

This situation is dynamically stable: the new spirals are dominated by the faster spiral on the right-hand side of the field and this dominant spiral pushes the other spirals towards the edge of the field (due to spiral competition, see Maselko and Schowalter 1991; Boerlijst and Hogeweg 1991b), where they disappear. New spirals are generated by the colliding and breaking of subsequent waves of the dominant spiral. If the drop of a gradient is too small a spiral will not break up. Note that the steepness of the gradient is not the critical factor. The situation is analogous to that of the mammalian intestine (see e.g. Winfree 1980), where the intrinsic frequency of peristaltic contractions at the stomach end is faster than that at the anus end, and thus some of the peristaltic waves fail to propagate and break.

3.2. Spiral drift

If the centre of the spiral wave is situated within the gradient a second phenomenon can be observed: the spiral will drift on the gradient. In Fig. 4 this phenomenon is visualised. The gradient is from ∇i : $\delta_i = 0.05$ at the middle to ∇i :

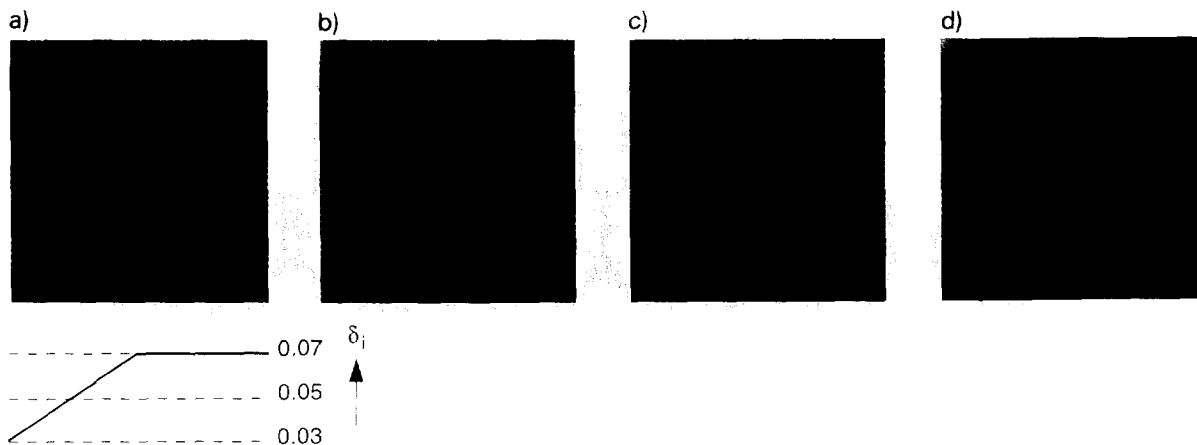


Fig. 3. Spiral break-up in the direction of slower rotation. The right-hand side of the field has a homogeneous decay-rate of ∇i : $\delta_i = 0.07$ and starting from the middle to the left-hand side there is a smooth gradient from ∇i : $\delta_i = 0.07$ to ∇i : $\delta_i = 0.03$. The diffusion rate is $D = 0.04$. Other parameters, numerics and grey scale are as in Fig. 2. We checked scaling up to 200×200 elements with $D = 0.16$ and a time step of 0.01, and found identical results. (a) Abundance of species X_1 after 2,000 time steps. (b) After 7,620 time steps. (c) After 8,500 time steps. (d) After 35,000 time steps.

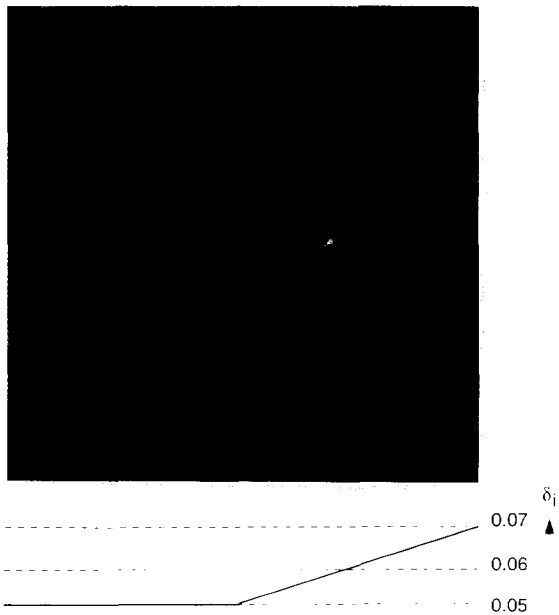


Fig. 4. Spiral drift in the direction of faster rotation. The left-hand side of the field has a homogeneous decay rate of $\nabla i: \delta_i = 0.05$ and starting from the middle of the field on the right-hand side there is a smooth gradient from $\nabla i: \delta_i = 0.05$ to $\nabla i: \delta_i = 0.07$. The diffusion rate is $D = 0.04$. Other parameters, numerics and grey scale are as in Fig. 2. A single spiral was initialised with the spiral tip at the position indicated by the arrow. The white dots indicate the positions of the spiral tip after every 20 rotations. The abundance of species X_1 after 101,400 time steps is shown.

$\delta_i = 0.07$ at the right; in this case the left side of the field is homogeneous at $\nabla i: \delta_i = 0.05$. The spiral begins to move at an angle in the direction

of faster rotation (note that the spiral would drift downwards if it were rotating clockwise instead of counter-clockwise). We think this direction of drift is caused by the increase in core size in the region of faster rotation. The precise mechanism, however, is not yet fully understood. Drift of spirals in the direction of faster rotation has been observed before (e.g. Mikhailov et al. 1994) although in most cases spirals drift in the direction of slower rotation (e.g. Rudenko and Panfilov 1983; Markus et al. 1992). The final outcome of this experiment will be that the centre of the spiral drifts off the field, resulting in the extinction of most species and loss of catalysis. This instability can be overcome by incorporating the full gradient in the field namely from $\nabla i: \delta_i = 0.03$ on the left to $\nabla i: \delta_i = 0.07$ on the right. In that case new spirals will be created as a result of break-up before the dominant spiral drifts off the field. After the loss of the dominant spiral the fastest remaining spiral will become dominant and it will start to drift to the right. In this manner a dynamic equilibrium will be maintained.

3.3. Radial gradient: dynamic equilibrium

In the case of a radial gradient another type of stable dynamic equilibrium will be attained. On the radial gradient of Fig. 5, both spiral drift and

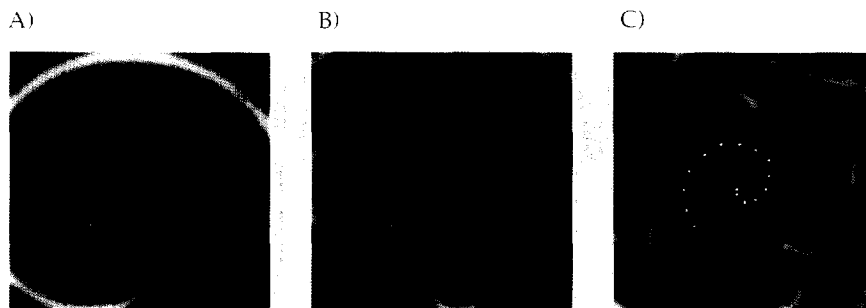


Fig. 5. Drift, break-up and anchoring of an initial single spiral on a radial gradient. There is a smooth gradient from $\nabla i: \delta_i = 0.07$ in the middle of the field to $\nabla i: \delta_i = 0.03$ in the corners. The diffusion rate is $D = 0.04$. Other parameters, numerics and grey scale are as in Fig. 2. The white dots indicate the positions of the spiral tip after every 10 rotations. (A) 2,500 time steps after initialisation a single spiral has developed. (B) After 10,900 time steps this spiral has formed peripheral break-up spirals. (C) After 139,100 time steps the dominant spiral has anchored in the region of fastest rotation and a dynamic equilibrium is reached.

spiral break-up take place. The single spiral in Fig. 5A will drift (with a radial angle) towards the region of fastest rotation. In approaching the centre the spiral speeds up and in Fig. 5B this has resulted in a break-up into new spirals in the periphery. In Fig. 5C the dynamic equilibrium of the system is reached: the initial spiral has anchored in the middle of the field and there are some “break-up” spirals in the periphery. Note that the dominant spiral in the middle prevents the break-up spirals from drifting to the middle. There is a continuous renewal of break-up spirals, analogous to the situation in Fig. 3D.

4. Strong parasites: regenerative power

Figs. 6A–D (colour plates) show what happens when a strong parasite invades a radial gradient. In plate 6A the centre of the dominant spiral of Fig. 5C is infected with a parasite. The parasite is competing with species 1, as depicted in Fig. 1B. It receives 10% more catalysis than species 1, but it does not give any catalysis and all other parameters are identical to species 1. The centre of the dominant spiral turns out to be the best possible place for a parasite to start, for all other invading parasites will be pushed out quickly by the dominant spiral. In plate 6B, after a short time, the parasite has killed the centre of the dominant spiral and now it is “riding” on the last wave of species 2, its catalyst. It turns out that most break-up spirals do not have a domain and therefore the parasite can get into the centre, which implies that the spiral will be “killed”. Plate 6C shows that one break-up spiral centre on the upper left-hand side of the field has escaped the first attacking wave of the parasites. In most of the field the parasite has now completely replaced the hypercycle and it has reached its non-catalytic carrying capacity. Finally, in plate 6D, the remaining spiral turns out to be stronger than the parasite. This spiral will completely push out all parasites. Furthermore, it will drift to the centre and it will generate new

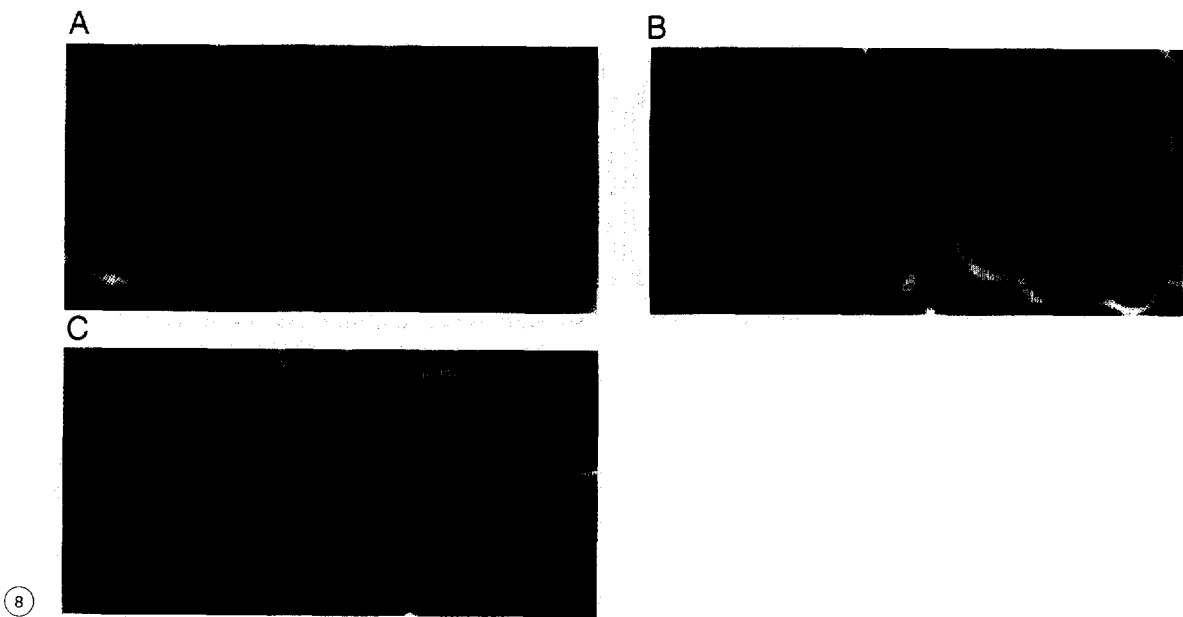
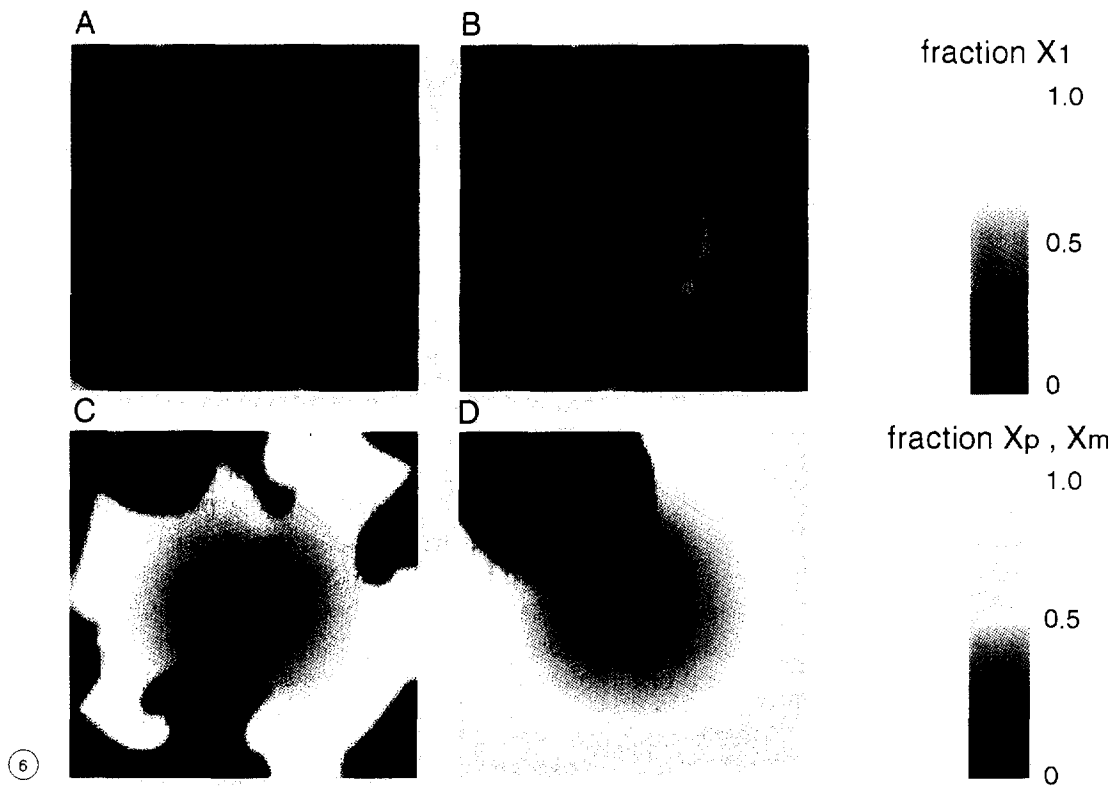
break-up spirals and thus the dynamic equilibrium will be restored completely. This re-establishment of the dynamic equilibrium after a parasite invasion does not happen in a homogeneous situation (Boerlijst and Hogeweg 1991a), for in that case a “killed” spiral will be lost for ever. We conclude that a spatial gradient can supply regenerative power to the hypercycle spirals.

In fact the situation of the hypercycle facing a parasite invasion in plate 6A is rather critical. Most break-up spirals do not have a domain of their own and therefore chances are high that the first parasite wave will reach the centre of all break-up spirals and thus the parasite will win. However, the parasite resistance can be enhanced by increasing the length (or steepness) of the gradient, so that the field contains many more break-up spirals. Furthermore, in a situation of multiple gradients, a gradient that is lost to a parasite can be re-invaded by spirals from an adjacent gradient. This multiple gradient situation has more intriguing features, which will be discussed in the following section.

5. Multiple fast regions: “sub-neutral selection”

In the case of multiple regions of fast rotation typically each of the regions will accumulate a dominant spiral. Fig. 7A shows such a case of two identical radial gradients, shortly after a random initialisation. After a while, in Fig. 7B, each fast region has attracted a spiral that dominates the local gradient. These dominant spirals are unable to force their period into the region of the other gradient; instead there is break-up of spirals in the periphery. This implies that the two dominant spirals are effectively disconnected by the gradient.

In plate 8A all molecules of species 1 which are near the centre of the dominant spiral on the right-hand side of Fig. 7B are replaced by molecules of a mutant species. The mutant only differs from species 1 in that it decays 30% more



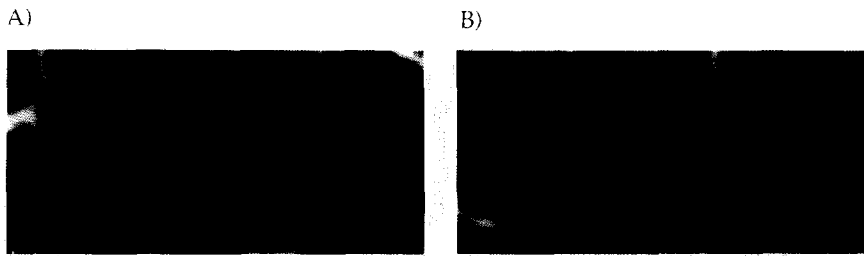


Fig. 7. Multiple gradients. Two gradients identical to the gradient of Fig. 5 are simulated on a field of 200×100 elements. As a starting pattern each grid point is assigned a random species and this species is set at its carrying capacity ($1 - \delta_i/\rho_i$). (A) After 3,000 time steps many spiral waves have developed. (B) After 100,000 time steps a dynamic equilibrium is reached in which each region of fast rotation has attracted a spiral that dominates the local gradient.

slowly. In plate 8B it turns out that the mutant quickly takes over the whole domain of the dominant spiral. It has also invaded some of the break-up spirals on the left gradient. It takes over these spirals because locally the mutant is much stronger than species 1. However, in plate 8C, in the long run the mutant species is restricted to the right gradient, whereas species 1 stays on the left gradient and this situation is stable in time.

Measurements of rotation speed show that the dominant spiral containing the mutant rotates at a slightly slower speed than the spiral containing species 1. In a situation without a gradient this would result in a slow increase of the domain of the faster rotating spiral (Boerlijst and Hogeweg 1991b; Maselko and Schowalter 1991). The gradient however disconnects the spirals in that the faster spiral is unable to force its period through the gradient. Therefore, in a multiple gradient situation, spirals with different rotation speeds can coexist. In fact the situation of multiple fast regions creates an environment in which there is what we call “sub-neutral selection”. In the situation of plate 8A any mutant creating a spiral

that rotates at a speed reasonably close to the period of the spiral with species 1 will accumulate and coexist with species 1. The limits of this coexistence are when the decay rate of the mutant is about 35% slower than that of species 1 and when the decay rate is about 70% faster than that of species 1. Mutants with a decay rate that is 35% slower than species 1 decay so slowly that they do not become extinct between spiral arms and therefore they can invade the spirals containing species 1 and thus outcompete species 1. Mutants with a decay rate that is 70% faster than that of species 1 decay so fast that they destabilise the spiral. In this case the spiral rotates so slowly that it is outcompeted by the surrounding break-up spirals containing species 1. Any mutant with a decay rate within these limits will accumulate in the system.

6. Conclusions and discussion

In this study we have shown that two gradient phenomena, namely spiral break-up and spiral drift, can create a dynamic equilibrium for hy-

Fig. 6. Resistance to parasites. A parasitic species X_p is described in the text; all other parameters are as in Fig. 5. (A) Parasite invasion in the centre of the dominant spiral of Fig. 5C. (B) 10,000 time steps after infection the first wave of parasites infects most peripheral spiral centres. (C) After 30,000 time steps one spiral centre near the upper left corner has escaped the first attack wave of the parasite. (D) After 90,000 time steps the remaining single spiral is slowly outcompeting the parasite region.

Fig. 8. “Sub-neutral selection” in a multiple gradient situation. (A) In the situation of Fig. 7B the centre of the dominant spiral on the right gradient is infected with a mutant of species X_1 that has a 30% reduced decay rate. (B) After 20,000 time steps the mutant has overtaken the right gradient and it has infected some peripheral spirals on the left gradient. (C) After 50,000 time steps the right gradient is dominated by the mutant and the left gradient is dominated by species X_1 .

percycle spirals. In the case of a radial gradient this equilibrium consists of one dominant spiral that has anchored in the fastest region and break-up spirals in its periphery. When the equilibrium is disturbed, for instance by a strong parasite invasion, it will be completely restored as long as there is one spiral centre left. In a homogeneous situation spiral waves can also have regenerative power in the parameter region of “chaotic spirals” (see Boerlijst and Hogeweg 1991b; Hassell et al. 1991). However, these chaotic spirals are inherently vulnerable to parasites, because in that case the break-up is caused by the fact that concentrations between spiral arms do not go to zero. We have shown earlier (Boerlijst and Hogeweg 1991a, Boerlijst et al. 1993) that extinction between subsequent waves is necessary for selection at the level of spirals. Only in the case of a gradient can resistance to strong parasites and regenerative power of spirals be combined.

In the paper so far we have focused on decay gradients and on mutants that differ in their decay rate. Preliminary results suggest that the conclusions reported apply to any kind of gradient or mutant: the spirals drift into the region of faster rotation, there is spiral break-up if the drop in the gradient is large enough and in a multiple fast region situation there is sub-neutral selection. The drift towards the region of faster rotating spirals seems to depend on the relatively weak catalysis: in the case of much stronger catalysis the spirals will drift almost perpendicular to the gradient and they will only drift towards the region of faster rotation on a very long time-scale. We never observed drift in the opposite direction, i.e. drift towards slower rotation, although this is the common tendency in other excitable media (see e.g. Rudenko and Panfilov 1983; Markus et al. 1992).

In a multiple gradient situation the competition between spirals no longer occurs in a simple way. Dominant spirals in different fast regions cannot force their period into other regions. It is as if each spiral sits in its own local valley and in

order to compete in other valleys it first has to climb the hills surrounding it and in doing so it loses much of its competitive strength. The result is that spirals in different valleys can substantially differ in properties, and yet be unable to outcompete each other. This coexistence of different mutants increases the capacity for the accumulation of information within the system, although the different schemes hardly interact. The case of multiple gradients should not be mistaken for a case of multiple isolated good habitats. In fact the centres of the gradients should be considered as bad habitats, for the molecules decay fast in these regions. Furthermore, the gradients are only isolated due to the presence of the spiral waves. If, for instance, one gradient loses all spirals as a result of a parasite invasion, it will easily be re-invaded by spirals from adjacent gradients.

The implications of our results for (pre-biotic) RNA hypercycles are yet unclear. Currently a two-dimensional experimental system containing RNAs with a hypercyclic interaction structure is being developed (McCaskill, personal communication; building upon McCaskill and Bauer 1993). It will be exciting to find out whether this system will exhibit spiral waves or other self-structuring patterns such as the patchy patterns we observed in a hypercycle model with negative interactions (Boerlijst and Hogeweg 1995) or the self-replicating spots recently observed in a chemical model system (Lee et al. 1994). In this paper we have shown that a spatial gradient can enhance the persistence of self-structuring patterns, at least when these are spiral waves.

Acknowledgements

We thank Dr. B.N. Vasiev for discussing the mechanisms of spiral drift, and Ms. S.M. McNab for linguistic advice. The research was supported by the Foundation for Biophysics, which is subsidized by the Netherlands Organization for Scientific Research (NWO).

References

- Boerlijst, M.C. and Hogeweg, P. (1991a), Spiral wave structure in pre-biotic evolution: hypercycles stable against parasites, *Physica D* 48, 17–28.
- Boerlijst, M.C. and Hogeweg, P. (1991b), Self-structuring and selection, in: *Artificial Life II*, eds. C.G. Langton, C. Taylor, J.D. Farmer and S. Rasmussen, (Addison-Wesley, Redwood City) pp. 255–276.
- Boerlijst, M.C., Lamers, M.E. and Hogeweg, P. (1993), Evolutionary consequences of spiral waves in a host-parasitoid system, *Proc. R. Soc. London B* 253, 15–18.
- Boerlijst, M.C. and Hogeweg, P. (1995), Attractors and spatial patterns in hypercycles with negative interactions, *J. Theor. Biol.*, in press.
- Davidenko, J.M., Pertsov, A.V., Salomonsz, R., Baxter, W. and Jalife, J. (1992), Stationary and drifting spiral waves of excitation in isolated cardiac muscle, *Nature* 355, 349–351.
- Durrett, R. and Levin, S. (1994), The importance of being discrete (and spatial), *Theor. Pop. Biol.* 46, 363–394.
- Eigen, M. (1971), Self-organization of matter and evolution of biological macromolecules, *Naturwissenschaften* 58, 465–523.
- Eigen, M. (1992), *Steps Towards Life – A Perspective on Evolution* (Oxford Univ. Press, Oxford).
- Eigen, M. and Schuster, P. (1979), *The Hypercycle: A Principle of Natural Self-Organization* (Springer, Berlin).
- Eigen, M. and Schuster, P. (1982), Stages of emerging life – five principles of early organization, *J. Mol. Evol.* 19, 47–61.
- Hassell, M.P., Comins, H.N. and May, R.M. (1991), Spatial structure and chaos in insect population dynamics, *Nature* 353, 255–258.
- Hofbauer, J. and Sigmund, K. (1988), *The Theory of Evolution and Dynamical Systems* (Cambridge Univ. Press, Cambridge).
- Jahnke, W., Skaggs, W.E. and Winfree, A.T. (1989), Chemical vortex dynamics in the Belousov–Zhabotinsky reaction and in the two-variable Oregonator model, *J. Phys. Chem.* 93, 740–749.
- Lee, K.J., McCormick, W.D., Pearson, J.E. and Swinney, H.L. (1994), Experimental observations of self-replicating spots in a reaction–diffusion system, *Nature* 369, 215–218.
- Markus, M., Nagy-Ungvarai, Z. and Hess, B. (1992), Phototaxis of spiral waves, *Science* 257, 225–227.
- Maselko, J. and Showalter, K. (1991), Chemical waves in inhomogeneous excitable media, *Physica D* 49, 21–32.
- May, R.M. (1991), Hypercycles spring to life, *Nature* 353, 607–608.
- Maynard Smith, J. (1979), Hypercycles and the origin of life, *Nature* 280, 445–446.
- McCaskill, J.S. and Bauer, G.J. (1993), Images of evolution: origin of spontaneous RNA replication waves, *Proc. Natl. Acad. Sci. USA* 90, 4191–4195.
- McGehee, R. and Armstrong, R.A. (1977), Some mathematical problems concerning the ecological principle of competitive exclusion, *J. Differ. Eqns.* 23, 30–52.
- Mikhailov, A.S., Davydov, V.A. and Zykov, V.S. (1994), Complex dynamics of spiral waves and motion of curves, *Physica D* 70, 1–39.
- Rudenko, A.N. and Panfilov, A.V. (1983), Drift and Interaction of vortices in two-dimensional heterogeneous active media, *Stud. Biophys.* 98, 183–188.
- Toffoli, T. & Margolus, N. (1987), *Cellular Automata Machines* (MIT Press, London).
- Winfree, A.T. (1980), The geometry of biological time, *Biomathematics* 8, 325–329.
- Yamaguchi, T. and Müller, S.C. (1991), Front geometries of chemical waves, *Physica D* 49, 40–46.